nature communications

Article

https://doi.org/10.1038/s41467-025-66569-z

Scalable reductive deuteration of (Hetero) Aryl chlorides with D_2O

Received: 18 August 2025

Accepted: 11 November 2025

Published online: 20 November 2025

Check for updates

Yu-Qiu Guan[1], Tian-Zhang Wang[1], Muhammad Bilal[1], Xin-Ru Tan[1], Lutz Ackermann[2] ✉ & Yu-Feng Liang[1] ✉

Deuterated compounds serve as powerful tools for investigating reaction mechanisms, tracing molecular pathways, as well as enhancing properties in medicinal and materials science. Herein, we report a nickel-catalyzed deuterodehalogenation of abundant yet inert aryl chlorides, enabling direct access to deuterated (hetero)arenes using D_2O as the exclusive, economical deuterium source. This reductive cross-coupling strategy overcomes traditional limitations of aryl chlorides and operates under mild conditions. This protocol delivers products with a high degree of deuterium incorporation across a broad range of (hetero)aryl substrates. It also exhibits excellent functional group tolerance and tolerates various sensitive functional groups including anilines, phenols, and organoboron derivatives. A variety of deuterated products have been efficiently prepared via site-selective chlorination intermediates. Moreover, the method is readily scalable to the kilogram level. Extensive mechanistic studies have been carried out to provide insights into the non-radical Ni^{I}/N^{III} catalytic cycle. The simplicity, cost-effectiveness, and scalability of this approach make it highly attractive for applications in drug discovery, mechanistic studies, and metabolic research.

Deuterium is a cost-effective and nonradioactive isotope of hydrogen that shares similar chemical properties with hydrogen in specific reactions[1]. Deuterated compounds are widely used in mechanistic research for isotope labeling, quantitative analysis, pharmacokinetic analysis, and other research domains[2–10]. In 2017, the U.S. Food and Drug Administration (FDA) reached a significant milestone by approving Austedo (deutetrabenazine) as the first deuterated drug. Since then, over 20 therapeutic compounds incorporating deuterium have progressed through various stages of clinical trials[11–14]. In recent years, deuteration has become a popular method for the discovery of new drugs. Notably, in 2022, the FDA approved deucravacitinib as an innovative de novo deuterated medication[15–17]. By harnessing the unique biological properties of deuterium, its application in medicine offers significant potential to enhance drug absorption, distribution, metabolism, and elimination. It also minimizes the adverse effects often seen with non-deuterated pharmaceuticals[18]. Impressively, following the COVID-19 pandemic, the number of scientific publications mentioning "deuteration" has steadily increased. Additionally, more than 20 deuterated drugs and biomarkers have been utilized in efforts to combat the pandemic. Therefore, developing deuteration methods that are green, efficient, economical, and broadly applicable is essential (Fig. 1A).

The choice of aryl halides as starting materials for deuteration is influenced by their reactivity hierarchy. Aryl bromides and iodides are generally preferred owing to their high reactivity in coupling reactions. In contrast, aryl chlorides, although inexpensive and abundant, have historically been underutilized owing to their poor reactivity in early synthetic steps and their limited potential for structural diversification[19]. Deuterated water (D_2O) further enhances practicality as a deuterium source, offering the lowest cost and superior storage stability, making it ideal for industrial or high-throughput deuteration (Fig. 1B). Unlocking the deuteration potential of aryl chlorides remains a key challenge, as traditional metal-halide exchange approaches, often employing strong bases like n-butyllithium to generate

[1]School of Chemistry and Chemical Engineering, Shandong University, Jinan, China. [2]Institut für Organische und Biomolekulare Chemie, Georg-August-Universität-Göttingen, Tammannstraße 2, Göttingen, Germany. ✉e-mail: Lutz.Ackermann@chemie.uni-goettingen.de; yfliang@sdu.edu.cn

https://doi.org/10.1038/s41467-025-66569-z

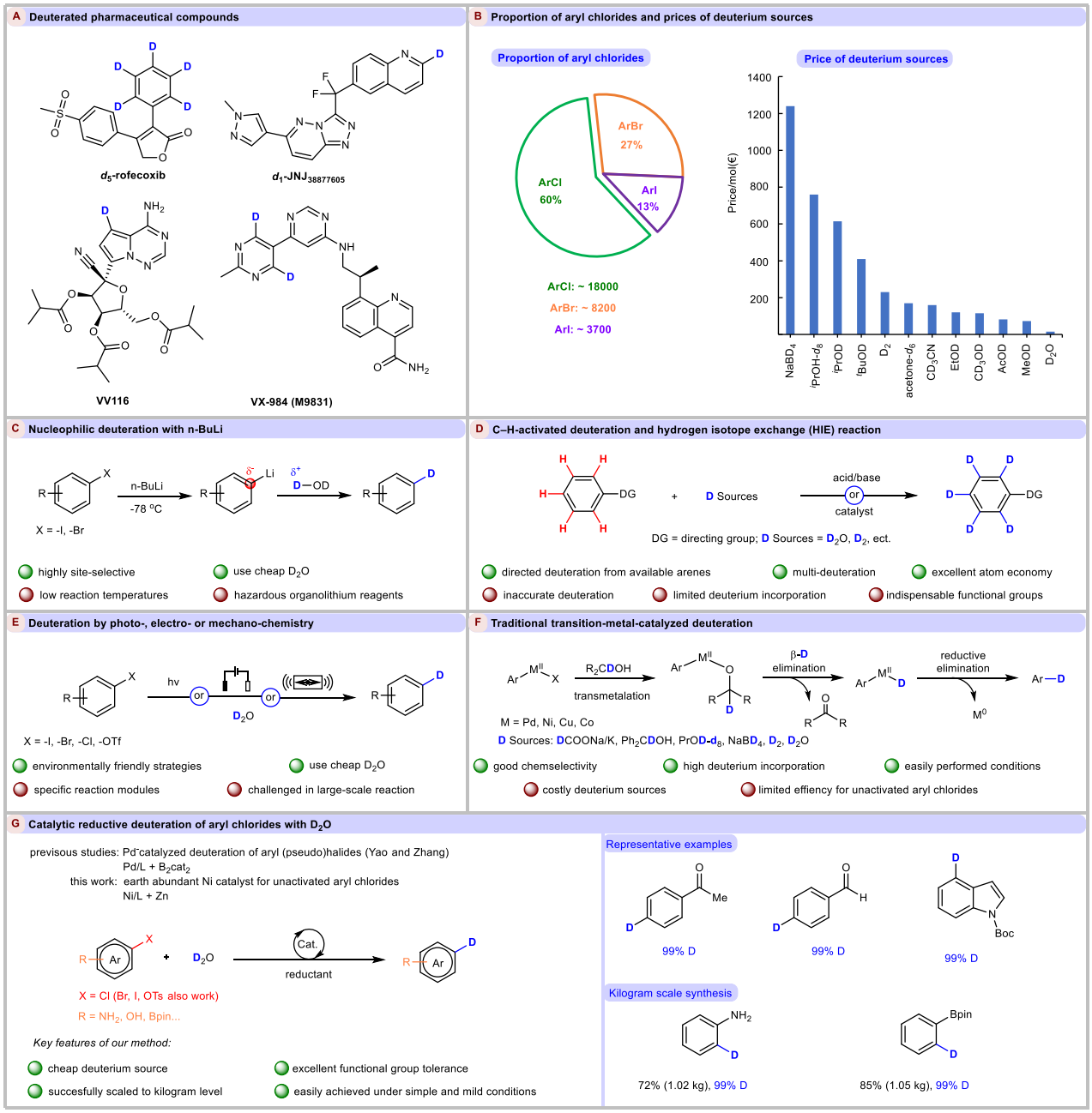

Fig. 1 | Background of deuteration reactions. A Deuterated pharmaceutical compounds. **B** Proportion of aryl chlorides and prices of deuterium sources. **C** Nucleophilic deuteration with a strong base. **D** Hydrogen isotope exchange (HIE) reaction. **E** Deuteration by photo- electro- or mechano-chemistry. **F** Traditional transition-metal catalyzed deuteration. **G** Catalytic reductive deuteration of aryl chlorides with D_2O.

organolithium intermediates, face significant limitations. These include harsh reaction conditions (low temperatures), the use of hazardous organolithium reagents, and inherently low efficiency with unactivated aryl chlorides[20–25] (Fig. 1C). To address these issues, C–H activation-based deuteration and hydrogen isotope exchange (HIE) strategies have emerged as alternatives for synthesizing deuterated aromatic/alkyl compounds, wherein functional groups are used for the activation of specific C–H bonds[26–52]. The activated C–H bonds are then exchanged with deuterium sources, yielding deuterated products. However, these methods require predefined functional groups for C–H bond activation, often resulting in incomplete or inaccurate deuteration, constraints that hinder their adoption in biochemistry (Fig. 1D). In parallel, visible light photoredox catalysis[53–61], organic electrochemistry[62–69] and mechanical-force-induced synthesis[70,71] have gained traction as sustainable synthetic tools, enabling mild reductive dehalogenation protocols with D_2O (Fig. 1E). These techniques involve the use of electrophilic reagents to induce the formation of the corresponding radicals or organometal reagents that react with deuterium sources to produce deuteration products. However, these approaches require specific photocatalytic, electrocatalytic reaction modules or mechanical force equipment, which restrict their applicability and feasibility. Furthermore, achieving high efficiency in reactions at the kilogram scale is a challenge for those strategies. Therefore, the development of a scalable and economical deuteration approach is crucial to facilitate the extensive use of this approach.

Given these challenges, transition metal[72,73], such as Pd[74–78], Ni[79], Cu[80] and Co[81,82], catalyzed deuteration using electrophilic aryl halides has attracted significant attention due to their inherent cost-effectiveness and easy availability. However, many methodologies typically rely on nucleophilic deuterated reagents (e.g., deuteroformates, α-deuterated alcohols, or $NaBD_4$), proceeded through mechanistic pathways involving β-D elimination and reductive elimination steps (Fig. 1F). Recently, Yao and Zhang reported an efficient palladium-catalyzed deuteration reaction of aryl (pseudo)halides with D_2O as deuterium source[83]. This efficient method for incorporating deuterium into drug molecules using cheap D_2O offers a practical strategy for late-stage deuteration. Despite the great achievements, the reliance on expensive palladium catalysts and limited reactivity with unactivated aryl chlorides warranted further investigation. To overcome these limitations, this study introduced a methodology employing earth abundant nickel as a catalyst and cheap deuterated water as the primary deuterium source to achieve the deuteration of inactivated aryl chlorides, within a reductive cross-coupling framework leading to higher yields during deuteration (Fig. 1G). This protocol offers several noteworthy advantages: a) utilization of D_2O as a cost-effective deuterium source; b) efficient synthesis of structurally diverse deuterated compounds featuring hydroxyl, amine, or boron functional groups, achieving excellent yields, broad substrate compatibility and exceptional chemoselectivity; c) easy scaling to the kilogram level, demonstrating its potential for application in industrial synthesis; and d) simple and mild conditions, which can be easily achieved in common chemical laboratories.

Results

We initiated our investigation by selecting 5-chloro-1,3-dimethoxybenzene (**1**) as the electrophile and D_2O as the deuterium source to evaluate the nickel-catalyzed reductive deuteration of aryl chlorides. Following a series of systematic investigations, the optimized conditions were established (Table 1). Under standard reaction conditions, using $NiCl_2$·DME (5 mol%) as the catalyst, 2,9-dimethylphenanthroline (L1, 6 mol%) as the ligand, zinc (3.0 equiv) as the reductant, and DMA as the solvent afforded the desired deuterated product **2** in 99% yield with more than 99% deuterium incorporation at room temperature over 12 h (entry 1). We found that P-ligands failed to afford the deuterated product (entries 2–3). Furthermore, reactions using alternative bidentate or tridentate N-ligands including 1,10-phen, bipyridine, and terpyridine afforded the product in lower yields with lower deuterium incorporation, indicating the ligand's critical role in this transformation (entries 4–10). Subsequent investigations revealed that other nickel(II) catalysts furnished product **2** in marginally reduced yield and with diminished deuterium incorporation (entries 11–13). Experiments with varying amounts of D_2O indicated that 5.0 equivalents of D_2O afforded the target product in high yield with excellent deuterium incorporation (entries 14–15). Control experiments underscored the crucial roles of the catalyst, ligand, and reductant. Omitting either the catalyst or reductant completely suppressed product formation, while omission of the ligand afforded the product in reduced yield (30%) and D-incorporation (27%) (entries 16–17).

To assess the generality of the deuteration method, a broad substrate scope was examined under the optimized conditions. A series of structurally diverse aryl chlorides representing electronically and sterically differentiated systems were evaluated to probe functional group compatibility (Fig. 2). Deuteration of polycyclic arenes yielded the deuterated isotopologues **3**–**4, 7**–**9** in good to excellent yields (75–96%) with excellent D-incorporation (95–99%). Moreover, the bromo-, iodo-, and pseudo-halogenated (tosylate) arenes similarly served as competent electrophilic partners under optimized conditions, providing corresponding isotopologue **4** in good yields. Aryl chlorides bearing acetyl, benzoyl, sensitive formyl, and ester groups were efficiently deuterated, providing the corresponding isotopologues **12**–**28** in 65–94% yields with 84–99% D-incorporations. It is noteworthy that this reaction is highly chemoselective, cleaving the Csp^2–Cl bond while tolerating the Csp^3–Cl bond (**28**). Selective deuteration of 3,5-dichloroethyl benzoate resulted in complete substitution of all chlorine atoms, affording the deuterated product **29** in 80% yield and 99% D-incorporation. Electronically diverse substituents including both electron-donating (e.g., **2, 32**) and electron-withdrawing groups (e.g., **5**–**6, 31, 33**) were well tolerated by the transformation. Generally, electron-poor substrates afforded consistently lower deuterium incorporation than their electron-rich counterparts, even with a larger amount of D_2O. Additionally, several protected anilines and phenols were successfully deuterated to isotopologues **34**–**37** in good yields and D-incorporation. This methodology extended to chlorinated heterocycles, delivering N-, O-, and S-containing isotopologues **38**–**47** in 67–90% yields with 85–99% D-incorporation. However, the nitro and aliphatic amine could not be compatible under the standard conditions (products **48, 49**).

We next applied the methodology to assess its robustness for substrates bearing strong electron-donating groups (phenols and anilines) as well as organoboron compounds and pharmaceutical agents. (Fig. 3). Deuteration of iodinated phenol substrates typically afforded isotopologues **50**–**53** in excellent yields (70–93%) with high D-incorporation (89–99%), though the para-substituted analog **50** exhibited lower D-labeling efficiency. Moreover, dihalogenated phenols bearing mixed halogens (Cl, Br, I) exhibited selective deuteration at the more reactive iodo sites, while chloro and bromo substituents remained intact in products **54** and **55**. We also found that para-, meta-, and ortho-chloroanilines **57**–**59** afforded the deuterated products in good yields. Anilines **61**–**64** exhibited higher yields and deuteration efficiency than **60** and **61**, potentially due to electronic effects. Remarkably, the ortho-position displayed a higher degree of D-incorporation than the para- and meta-positions. Subsequently, mixed-halogen substrates **62** and **63** displayed selective iodine deuteration while retaining chloro or bromo substituents. Notably, the reaction was successfully scaled up to 10 grams for ortho-deuterated phenol **51** and aniline **59**, providing the products in isolated yields of 89% and 80%, respectively, thus demonstrating its potential for industrial-scale deuterium labeling applications. For these electron-rich phenols and anilines, a reaction temperature of 80 °C was required to achieve good yields and deuterium incorporation. Notably, the developed methodology expresses tolerance to boron-containing groups, which are less frequently reported in traditional metal-catalyzed deuteration. Several aryl chlorides containing –Bpin and –Bcat afforded isotopologues **68**–**74** in excellent yields (61–92%) and D-incorporation (89–99%). Notably, complete deutero-dehalogenation of multi-halogen organoborons **75**–**77** proceeded efficiently, delivering consistently high yields (71–87%) and D-incorporation (98–99%). To demonstrate methodological robustness, late-stage deuteration was successfully applied to pharmaceutically relevant compounds. For instance, chlorpropham underwent efficient deuteration to afford **78** with high D-incorporation (80%). Clofibrate was similarly transformed to its deuterated analogue **79** with 99% D-incorporation. This protocol was further extended to fenofibrate and chloromezanone yielding isotopologues **80** and **81** with deuteration efficiency of 99% respectively. Furthermore, dehalogenative deuteration of esters derived from 2-chlorophenol and pharmacologically relevant carboxylic acids (gemfibrozil, naproxen, and probenecid) afforded deuterated drug derivatives **82**–**84** with 99% deuterium incorporation.

Furthermore, sequential reactions were conducted to synthesize deuterated substrates (Fig. 4). The process began with various (hetero) arenes as starting materials, which underwent highly efficient Jiao chlorination under straightforward conditions[84,85]. The resulting chlorinated intermediates were then subjected to dehalogenative deuteration under our standard reaction conditions, yielding the

https://doi.org/10.1038/s41467-025-66569-z

Table 1 | Investigation of reaction conditions[a]

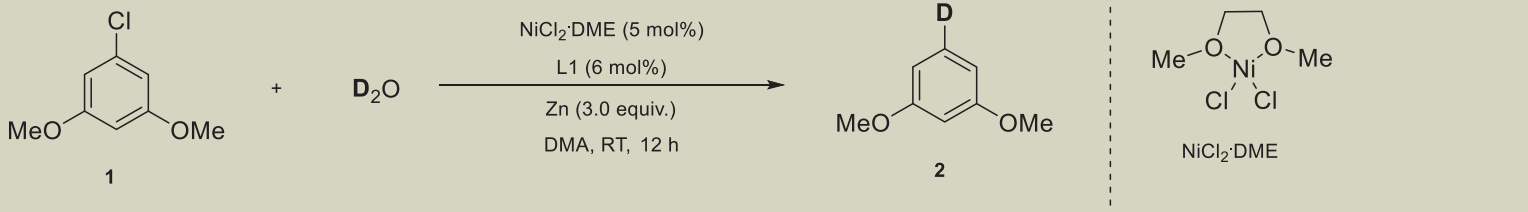

entry	Variation of optimal conditions	yield[b]	D-inc[c]
1	none	99%	> 99%
2	PCy_3 instead of L1	n.d.	--
3	PPh_3 instead of L1	trace	--
4	L2 instead of L1	82%	90%
5	L3 instead of L1	71%	57%
6	L4 instead of L1	79%	58%
7	L5 instead of L1	53%	50%
8	L6 instead of L1	57%	52%
9	L7 instead of L1	41%	47%
10	L8 instead of L1	n.d.	--
11	$NiCl_2$ instead of $NiCl_2$·DME	87%	90%
12	$NiBr_2$·DME instead of $NiCl_2$·DME	91%	95%
13	$Ni(acac)_2$ instead of $NiCl_2$·DME	68%	85%
14	D_2O (3.0 equiv)	72%	95%
15	D_2O (5.0 equiv)	99%	>99%
16	w/o ligand	30%	27%
17	w/o Cat. or w/o Red.	n.d.	--

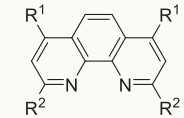

L1: R^1 = H, R^2 = Me
L2: R^1 = R^2 = H
L3: R^1 = Me, R^2 = H
L4: R^1 = Ph, R^2 = H

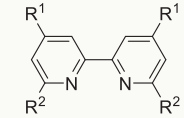

L5: R^1 = R^2 = H
L6: R^1 = H, R^2 = Me
L7: R^1 = R^2 = Me

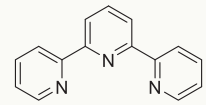

L8

[a]Reaction conditions: **1** (0.2 mmol), D_2O (2.0 mmol), catalyst (5 mol %), ligand (6 mol %), reductant (3.0 equiv.), and DMA (1.0 mL) at room temperature for 12 h under N_2. [b]Determined by GC–MS analysis of the crude reaction mixture using benzophenone as an internal standard. [c]Deuterium incorporation was determined by ^1H NMR analysis.

https://doi.org/10.1038/s41467-025-66569-z

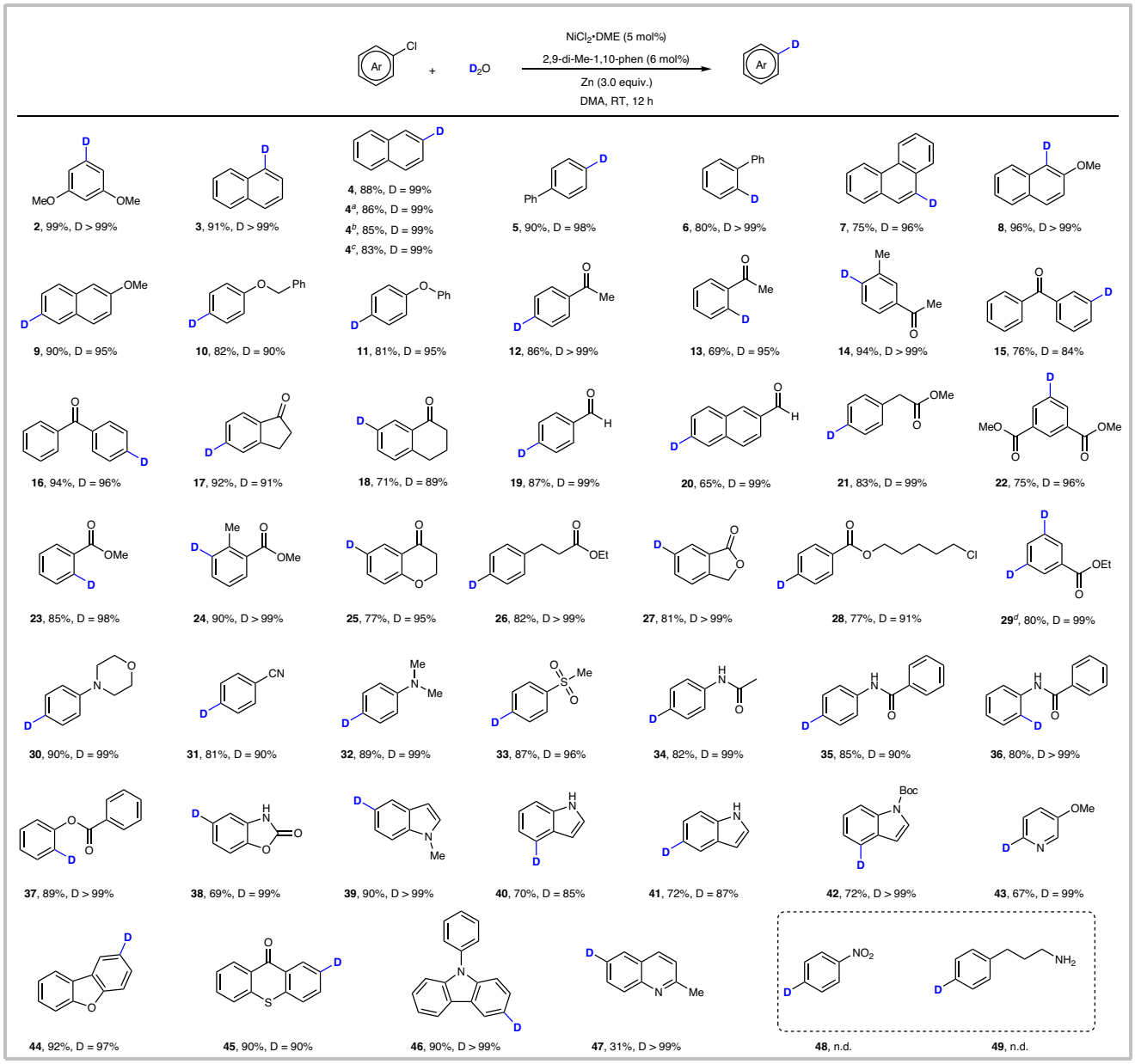

Fig. 2 | Scope of deuteration of aryl chlorides with deuterium oxide. Reaction conditions: aryl chlorides (0.2 mmol), D_2O (1.0 mmol), $NiCl_2$·DME (5 mol %), 2,9-di-Me-1,10-phen (6 mol %), Zn (3.0 equiv.), and DMA (1.0 mL) at RT for 12 h under N_2. [a]–I instead of –Cl. [b]–Br instead of –Cl. [c]–OTs instead of –Cl. [d]Zn (6.0 equiv.), D_2O (2.0 mmol). Isolated yields.

corresponding deuterated products in isolated yields ranging from 62% to 96%, with deuterium incorporation between 86% and 99% (**85**–**95**). This strategy demonstrates that a range of (hetero)arenes can be site-selectively deuterated through the combination of the useful Jiao chlorination and our dehalogenative deuteration protocol.

Encouraged by the successful milligram-scale reactions in dehalogenative deuteration, kilogram-scale reactions were then designed to demonstrate the potential of this approach for practical synthesis (Fig. 5). Two deuterated products containing active substituents such as organoboron and amine derivatives were selected for the synthesis. In previous studies, costly reaction conditions were required for the synthesis of benzen-2-*d*-amine[86]. This study utilized cheaper conditions to synthesize deuterated anilines on a kilogram scale within 16 hours, achieving a 72% yield (1.02 kg) with over 99% D-incorporation (Fig. 5A). Furthermore, previous studies indicated that expensive palladium catalysts and deuterium sources are necessary for the synthesis of 2-deuterated organoboron[78]. Scaled deuteration afforded 1.05 kg of the boron-functionalized isotopologue in 85% isolated yield with > 99% D-incorporation via simple filtration, extraction and distillation, demonstrating its industrial viability (Fig. 5B). To our delight, this kilogram-scale synthesis was successfully executed with a lower catalyst loading (2.5 mol% Ni, 3.0 mol% ligand), achieving excellent deuterium incorporation and a slight reduction in yield within 36 hours, thus establishing a viable process for industrial-scale deuterium labeling.

To gain further insight into the reaction mechanism, several relevant experiments were conducted under the standard reaction conditions (Fig. 6). Radical trapping studies employing (1-cyclopropylvinyl)benzene as a radical clock yielded exclusively the non-rearranged deuterated product in 77% isolated yield (Fig. 6A, up).

https://doi.org/10.1038/s41467-025-66569-z

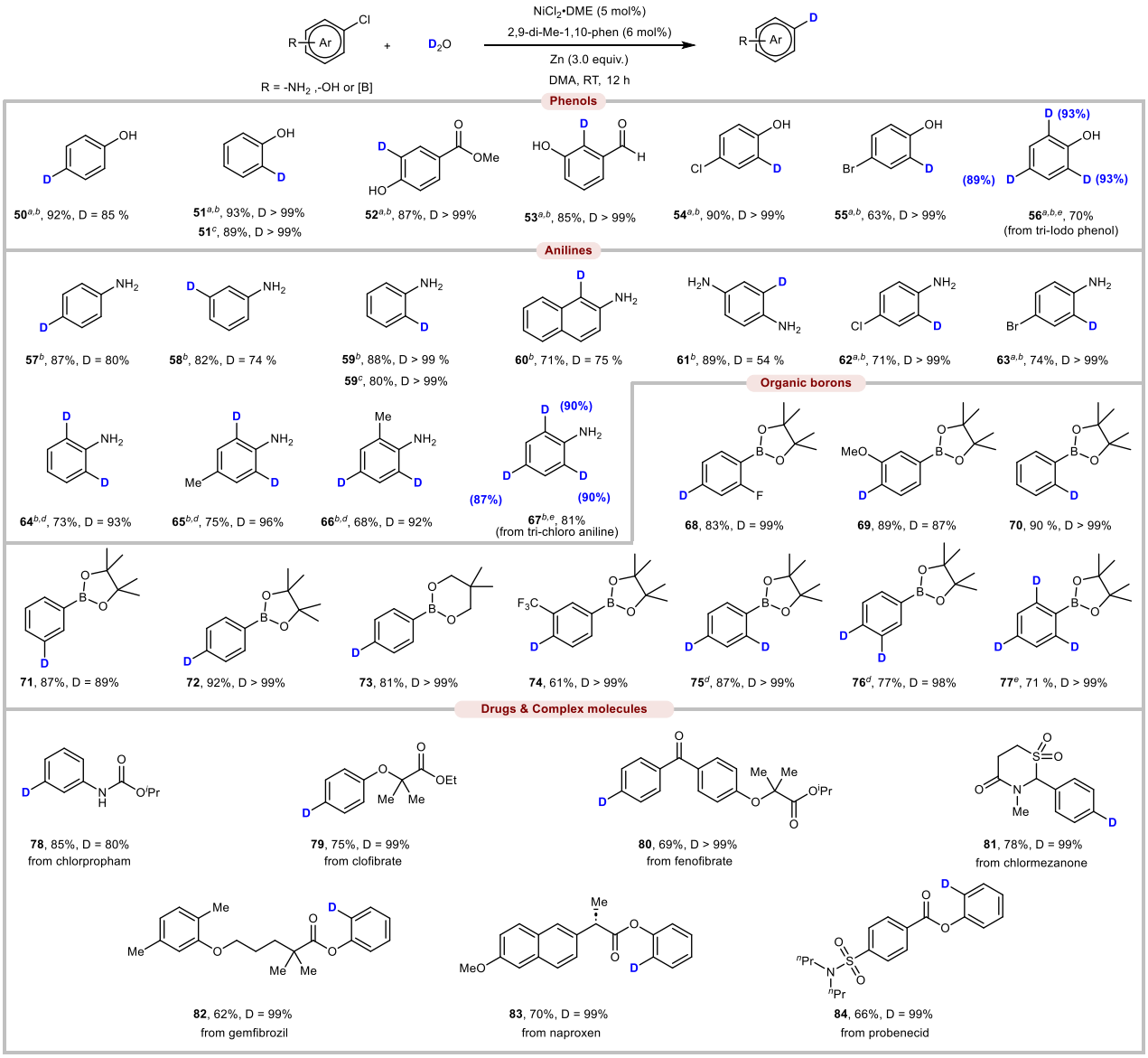

Fig. 3 | Deuteration of aryl chlorides with active functional groups. Reaction conditions: aryl chlorides (0.2 mmol), D_2O (2.0 mmol), $NiCl_2$·DME (5 mol %), 2,9-di-Me-1,10-phen (6 mol %), Zn (3.0 equiv.), and DMA (1.0 mL) at RT for 12 h under N_2. Isolated yields. [a]−I instead of −Cl. [b]80 °C instead of RT. [c]10 gram-scale reaction yields. [d]Zn (6.0 equiv.), D_2O (4.0 mmol). [e]Zn (9.0 equiv.), D_2O (6.0 mmol).

The observed cyclopropane ring integrity indicates the absence of free radical intermediates under standard reaction conditions. In addition, 1-chloro-2-(4-methylpent-3-en-1-yl)benzene was tested as the aryl halide radical trap. The absence of cyclization products further ruled out the possibility of an aryl radical intermediate (Fig. 6A, down)[87]. Then, we used a series of reductants, including heterogeneous powder reductants, such as Mn and Fe, as alternatives to Zn. The reaction using Mn as the reductant yielded a significant amount of the desired product, albeit lower than with Zn, suggesting that the formation of an organozinc intermediate is not essential for the reaction (Fig. 6B, entries 1–3)[88]. Reactions with TDAE [tetrakis(dimethylamino)ethylene] or B_2pin_2 as organic reductant also produced the deuterated product, though in low yields, further supporting that an organozinc intermediate is not required for the reaction (Fig. 6B, entries 4 and 5). To exclude deeper organozinc intermediate involved, sequential mechanistic studies were performed (Figs. 6C and 6D). Firstly, D_2O quenching experiments were conducted. If organozinc was formed as intermediate, detectable deuteration product would be immediately generated when D_2O was added. However, GC–MS analysis revealed trace amount of deuteration product, again suggesting that an organozinc reagent is not involved in this reaction (Fig. 6C). Secondly, a Pd-catalyzed Negishi-type coupling reaction was employed to probe organozinc intermediates[89]. No coupling products were observed, further confirming that organozinc reagents do not participate in this process (Fig. 6D)[90]. These findings collectively ruled out organozinc involvement in the reaction mechanism. An alternative mechanistic hypothesis was that zinc reacts with D_2O to produce D_2, which could act as a reductant for the nickel catalyst[91]. To validate this proposed pathway, a hydrogen reduction experiment was performed. The absence of protonated products confirmed that hydrogen generation via this mechanism is negligible (Fig. 6E). Further mechanistic insights were obtained through kinetic isotope experiments. Competitive

https://doi.org/10.1038/s41467-025-66569-z

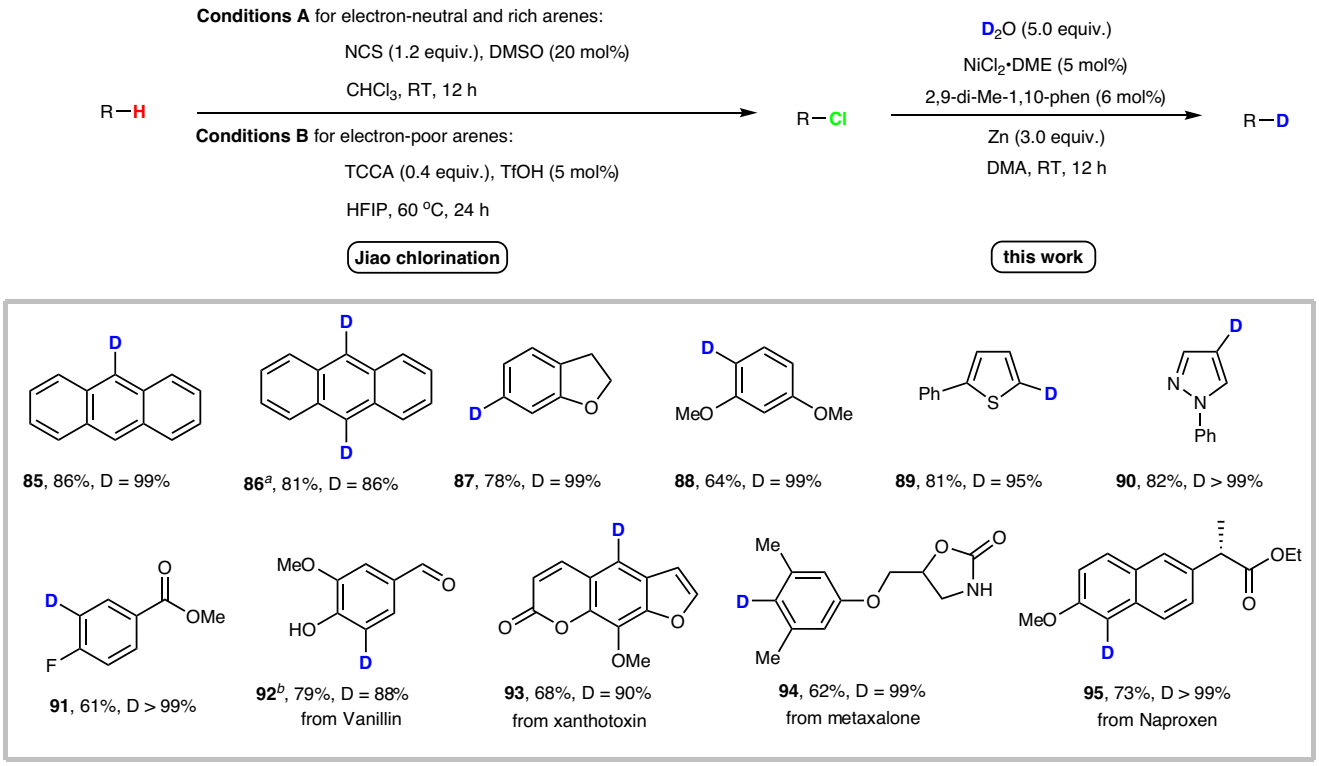

Fig. 4 | Stepwise hydrogen isotope exchange via Jiao chlorination. [a]Zn (6.0 equiv.), D_2O (2.0 mmol). [b]80 °C instead of RT. Isolated yields.

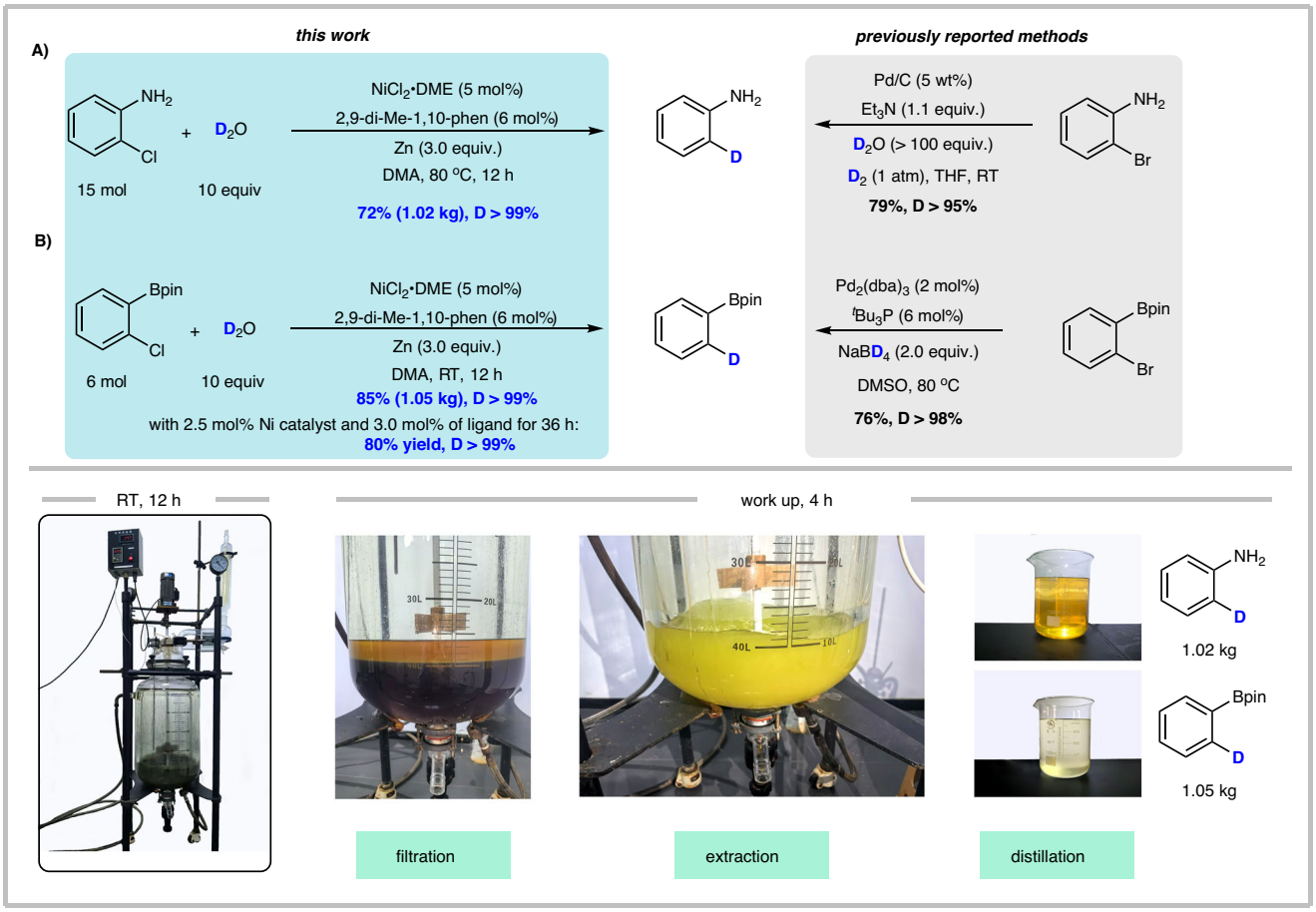

Fig. 5 | Kilogram-scale synthesis. A Preparation of benzen-2-*d*-amine in kilogram-scale. **B** Preparation of 4,4,5,5-tetramethyl-2-(phenyl-2-*d*)-1,3,2-dioxaborolane in kilogram-scale.

https://doi.org/10.1038/s41467-025-66569-z

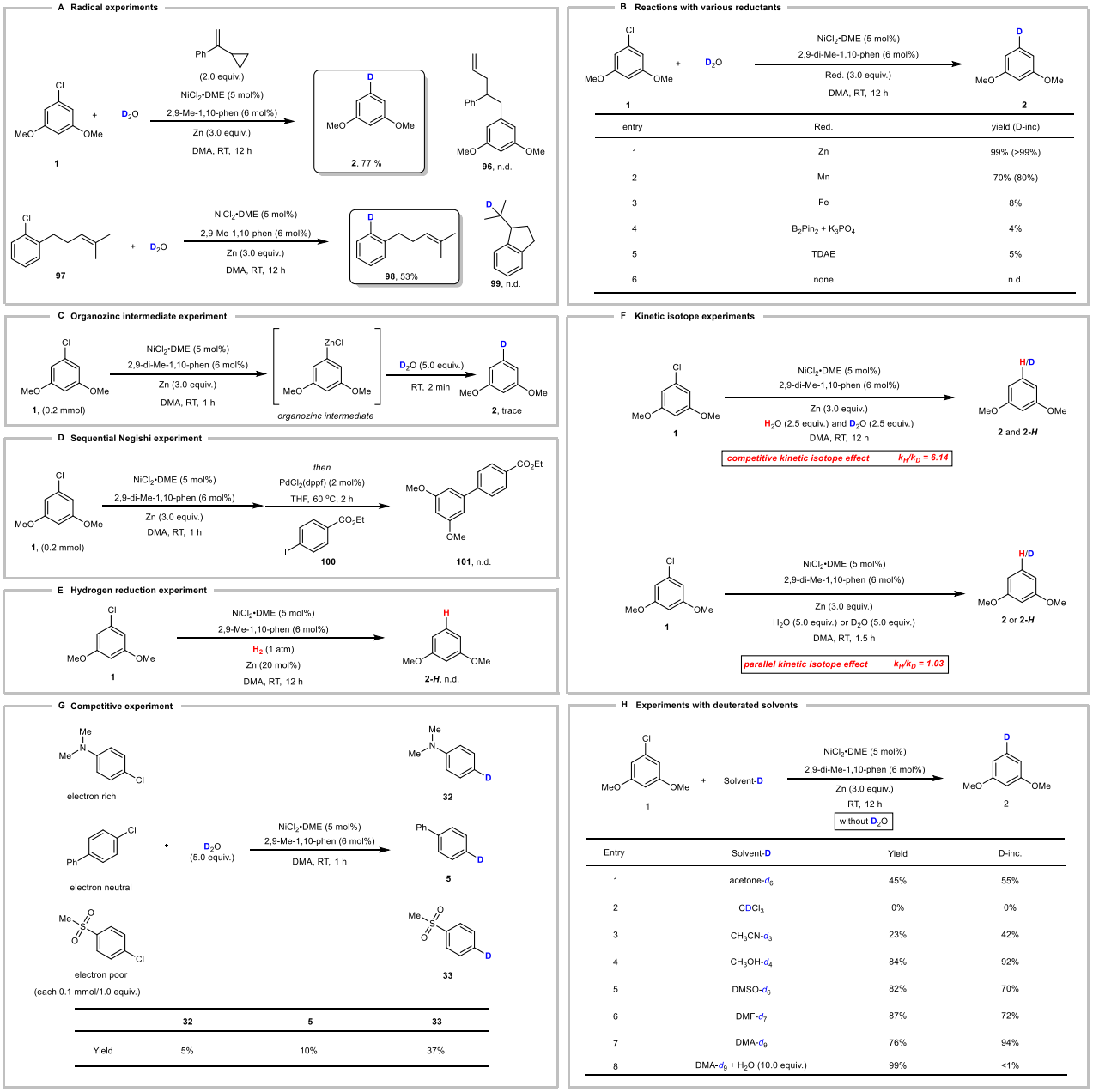

Fig. 6 | Mechanistic experiments. A Radical experiments. **B** Reductant scope experiments. **C** Organozinc intermediate experiment. **D** Sequential Negishi experiment. **E** Hydrogen reduction experiment. **F** Kinetic isotope experiments. **G** Competitive experiment. **H** Experiments with deuterated solvents.

kinetic isotope (KIE = 6.14) studies demonstrated that neither aryl radicals nor deuterium radicals participate in the reaction. Parallel experiments (KIE = 1.03) revealed that C–D bond formation is not the rate-determining step (Fig. 6F). Additionally, to investigate the influence of different substituent groups on reaction activity, competitive experiments were conducted using substrates bearing *N*,*N*-dimethyl, phenyl, and methylsulfonyl functionalities. The reaction results demonstrated that the methylsulfonyl-substituted substrate yielded a significantly higher deuterated product compared to its counterparts. This outcome strongly suggests that electron-withdrawing groups may facilitate faster reaction rates than electron-donating groups (Fig. 6G). To further clarify the specific relationship between the solvent and deuterium incorporation, a series of deuterated solvents were tested as the deuteration source in the absence of D_2O (Fig. 6H). Experimental results revealed that protons inherent in the reaction solvent can partially influence the deuterium incorporation rate of the product, although the protons in solvent are much less reactive than water (entries 7–8, Fig. 6H). The incomplete deuteration may be due to the presence of trace amounts of water in the deuterated solvents. These findings serve as direct evidences that reduced deuterium incorporation for some products (**15, 18, 31, 45**) may arise from protonation with the solvent.

Kinetic studies were performed to elucidate the reaction mechanism (Fig. 7A). Firstly, a time-course study was conducted. The graph shows a gradual acceleration of the rate as the reaction progressed, followed by a gradual decline after 150 min. Detailed kinetic analysis through GC–MS yields highlighted a first-order dependence with respect to the concentration of $NiCl_2$·DME. In addition, a zeroth-order dependence on the concentration of aryl chloride and D_2O was observed, indicating that the conversion of an intermediate assembled

https://doi.org/10.1038/s41467-025-66569-z

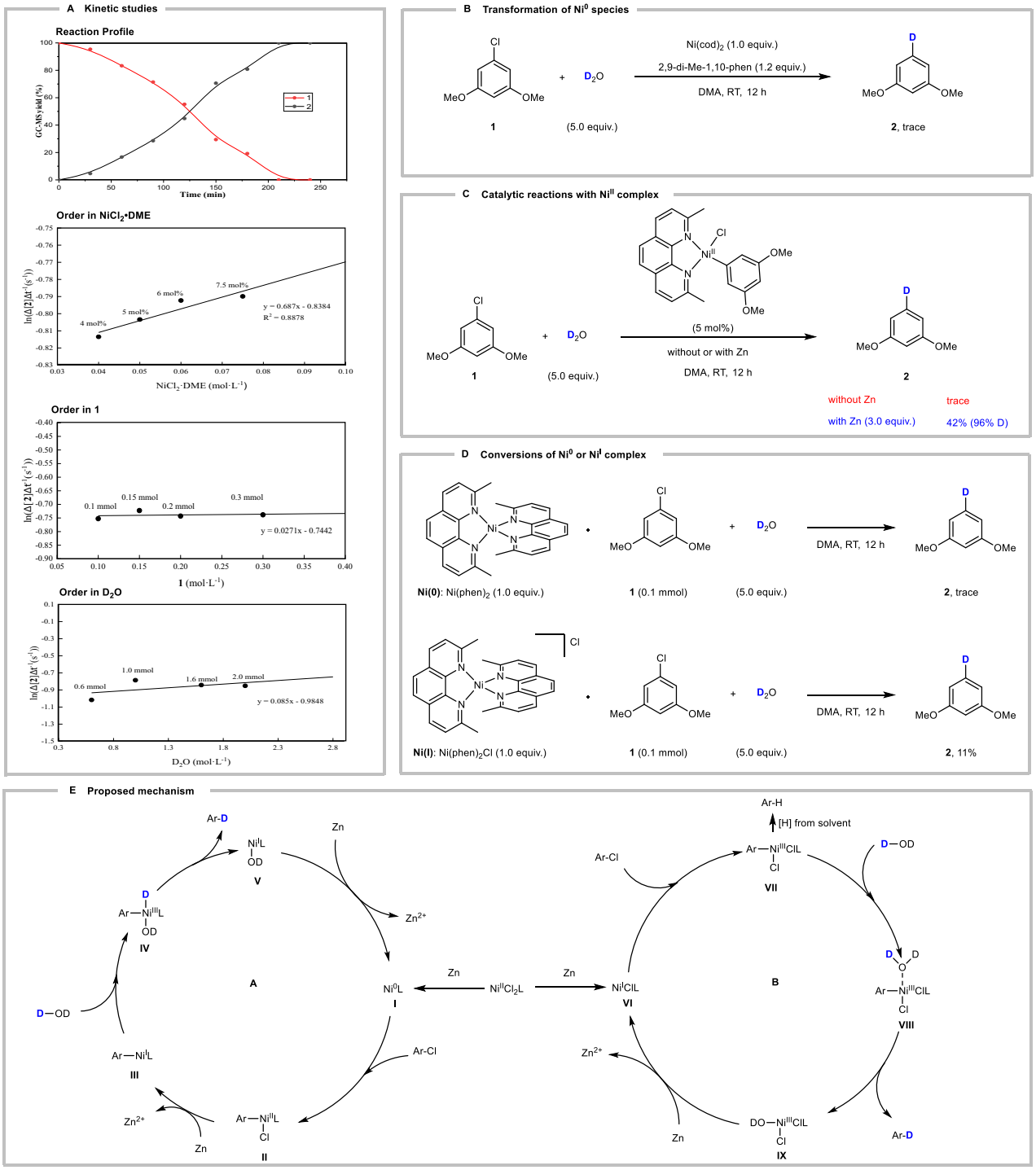

Fig. 7 | Intermediates studies and proposed catalytic cycle. A Kinetic studies. **B** Transformation of Ni^0 species. **C** Catalytic reactions with Ni^{II} complex. **D** Conversions of Ni^0 or Ni^I complex. **E** Proposed reaction mechanism.

from both the reagents and the Ni catalyst might be involved in the rate-determining step. To further elucidate the mechanism intermediate, we conducted the following experiments. First, we performed the reaction between **1** and stoichiometric amount of Ni^0 catalyst, specifically $Ni(cod)_2$, in the absence of Zn powder. Unfortunately, only trace amount of the desired deuterated product was observed, suggesting that Ni^0 might not the active catalyst species (Fig. 7B). To obtain further information, complex Ar–Ni^{II}(2,9-di-Me-1,10-phen)Cl was synthesized. This experimental design was guided by the hypothesis that zinc plays a critical role in reducing Ni^{II} to a nucleophilic $ArNi^I$ species, thereby facilitating the catalytic cycle. As shown in Fig. 7C, the addition of zinc powder significantly enhanced the product yield, directly supporting the hypothesis that zinc-mediated reduction of Ni^{II} to $ArNi^I$ is an essential step in the reaction pathway[92–96]. To further probe the involvement of nickel species, the Ni^0 and Ni^I complexes were synthesized using established methodologies[97] and subsequently reacted with D_2O. However, no deuterated products were detected when Ni^0 was employed as the

initial nickel catalyst (Fig. 7D, up). In contrast, the stoichiometric reaction of Ni^{I} complex with substrate **1** and D_2O furnished the desired deuteration product, although in 11% yield, indicating the Ni^{I} complex might be involved as a key intermediate (Fig. 7D, down). These results provided unambiguous evidence that Ni^{0} does not function as a key intermediate in this transformation. Consequently, the proposed mechanism involving Ni^{0} **I** underwent oxidative addition to form Ni^{II} **II**, followed by reduction to Ni^{I} **III**, which would undergo oxidative addition with deuterium oxide to give Ni^{III} intermediate **IV**[98], and finally reductive elimination to yield deuteration products and Ni^{I} **V** might be excluded (Fig. 7E, cycle A). Based on the aforementioned experimental results and literature reports[92–98], we propose a plausible reaction mechanism (Fig. 7E, cycle B). Initially, the Ni^{I} complex **VI** could be formed under reductive conditions, followed by oxidative addition of aryl chloride to yield Ni^{III} complex **VII**. The resulting intermediate is then protonated by D_2O via a Ni(III)-D_2O species **VIII** to form the deuterated products. The competitive protonation with solvent would decrease the deuterium incorporation efficiency for some highly reactive substrates. Lastly, the active Ni^{I} complex **VI** is regenerated for further catalytic cycles via reduction of Ni^{III} complex **IX**.

Discussion

In summary, a versatile dehalogenation method was successfully established for readily accessible aryl chlorides using D_2O as the deuterium source under reductive conditions. This protocol entails reductive deuteration via oxidative addition and protonation through a Ni^{I} process. Our strategy offers a mild and efficient dehalogenative deuteration pathway for a range of inactivated (hetero) aryl chlorides with excellent functional group tolerance including sensitive phenol, anilines, formyl and boronated groups. Further, carbonyls, esters, amides, and diverse N/O/S-heterocycles remained intact under reaction conditions. More importantly, its applicability has been strongly demonstrated by reactions conducted on the kilogram scale. Notably, this robust strategy necessitates 5.0–10.0 equivalents of D_2O and can be performed at room temperature, leading to a high degree of deuterium incorporation. This rapid and cost-effective methodology for the synthesis of highly deuterium-labeled (hetero)aryl compounds holds significant potential for applications in drug development and metabolic studies. Overall, this approach employs a practical, safe, and cost-efficient deuteration strategy that delivers high-value deuterated compounds. Further investigation on reductive deuteration will be continuously explored in our group.

Methods

General procedure for the nickel-catalyzed deuteration

To a 10 mL Schlenk tube was added sequentially $NiCl_2$·DME (2.20 mg, 0.010 mmol), 2,9-dimethyl-1,10-phenanthroline (2.25 mg, 0.012 mmol), Zn powder (40.0 mg, 0.6 mmol). The vessel was evacuated and filled with argon (three times), DMA (0.50 mL) was added via syringe and the mixture was stirred at room temperature for 10 min. The deuterated water (20.0–40.0 mg, 1.0–2.0 mmol) was added, followed by the addition of aryl chloride (0.2 mmol) in one portion. DMA (0.50 mL) was subsequently added via syringe. The resulting solution was stirred for 12 h at room temperature. After this time, the crude reaction mixture was diluted with ethyl acetate (10 mL) and washed with water (2.0 mL × 3). The organic layer was dried over Na_2SO_4, filtered, and concentrated. The residue was purified by flash chromatography.

Data availability

The authors declare that all other data supporting the findings of this study, including experimental procedures and compound characterization, are available within the article and its Supplementary Information files. All data are available from the corresponding author upon request.

References

1. Prechtl, M. H. G. et al. Catalytic C–H bond activation at nanoscale Lewis acidic aluminium fluorides: H/D exchange reactions at aromatic and aliphatic hydrocarbons. *Chem. Eur. J.* **17**, 14385–14388 (2011).
2. Simmons, E. M. & Hartwig, J. F. On the interpretation of deuterium kinetic isotope effects in C–H bond functionalizations by transition-metal complexes. *Angew. Chem. Int. Ed.* **51**, 3066–3072 (2012).
3. Watile, R. et al. Intramolecular substitutions of secondary and tertiary alcohols with chirality transfer by an iron(III) catalyst. *Nat. Commun.* **10**, 3826–3834 (2019).
4. Marcus, D. M. et al. Experimental evidence from H/D exchange studies for the failure of direct C–C coupling mechanisms in the methanol-to-olefin process catalyzed by HSAPO-34. *Angew. Chem. Int. Ed.* **45**, 3133–3136 (2006).
5. Plesniak, M. P., Garduño-Castro, M. H., Lenz, P., Just-Baringo, X. & Procter, D. J. Amarium(II) folding cascades involving hydrogen atom transfer for the synthesis of complex polycycles. *Nat. Commun.* **9**, 4802–4810 (2018).
6. Konermann, L., Pan, J. X. & Liu, Y. H. Hydrogen exchange mass spectrometry for studying protein structure and dynamics. *Chem. Soc. Rev.* **40**, 1224–1234 (2011).
7. Meanwell, N. A. Synopsis of some recent tactical application of bioisosteres in drug design. *J. Med. Chem.* **54**, 2529–2591 (2011).
8. Palazzolo, A. et al. Efficient access to deuterated and tritiated nucleobase pharmaceuticals and oligonucleotides using hydrogen-isotope exchange. *Angew. Chem. Int. Ed.* **58**, 4891–4895 (2019).
9. Atzrodt, J., Derdau, V., Kerr, W. J. & Reid, M. Deuterium- and tritium-labelled compounds: applications in the life Sciences. *Angew. Chem. Int. Ed.* **57**, 1758–1784 (2018).
10. Roßmann, K. et al. Deuteration as a general strategy to enhance azobenzene-based photopharmacology. *Angew. Chem. Int. Ed.* **63**, e202408300 (2024).
11. Schmidt, C. First deuterated drug approved. *Nat. Biotechnol.* **35**, 493–494 (2017).
12. Pirali, T., Serafini, M., Cargnin, S. & Genazzani, A. A. Applications of deuterium in medicinal chemistry. *J. Med. Chem.* **62**, 5276–5297 (2019).
13. Mullard, A. Deuterated drugs draw heavier backing. *Nat. Rev. Drug Discov.* **15**, 219–221 (2016).
14. Ran, C.-K. & Yu, D.-G. Ready and label. *Nat. Rev. Chem.* **6**, 679–680 (2022).
15. Di Martino, R. M. C., Maxwell, B. D. & Pirali, T. Deuterium in drug discovery: progress, opportunities and challenges. *Nat. Rev. Drug Discov.* **22**, 562–584 (2023).
16. Katsnelson, A. Heavy drugs draw heavy interest from pharma backers. *Nat. Med.* **19**, 656–656 (2013).
17. Timmins, G. S. Deuterated drugs; updates and obviousness analysis. *Expert Opin. Ther. Pat.* **27**, 1353–1361 (2017).
18. Jansen-van Vuuren, R. D., Jedlovčnik, L., Košmrlj, J., Massey, T. E. & Derdau, V. Deuterated drugs and biomarkers in the COVID-19 pandemic. *ACS Omega* **7**, 41840–41858 (2022).
19. Alonso, F., Beletskaya, I. P. & Yus, M. Metal-mediated reductive hydrodehalogenation of organic halides. *Chem. Rev.* **102**, 4009–4092 (2002).
20. Ong, D. Y., Tejo, C., Xu, K., Hirao, H. & Chiba, S. Hydrodehalogenation of haloarenes by a sodium hydride–iodide composite. *Angew. Chem. Int. Ed.* **56**, 1840–1844 (2017).
21. Hokamp, T. et al. Radical hydrodehalogenation of aryl bromides and chlorides with sodium hydride and 1,4-dioxane. *Angew. Chem. Int. Ed.* **56**, 13275–13278 (2017).
22. Spiegel, D. A., Wiberg, K. B., Schacherer, L. N., Medeiros, M. R. & Wood, J. L. Deoxygenation of alcohols employing water as the hydrogen atom source. *J. Am. Chem. Soc.* **127**, 12513–12515 (2005).

23. Soulard, V., Villa, G., Vollmar, D. P. & Renaud, P. Radical deuteration with D_2O: catalysis and mechanistic insights. *J. Am. Chem. Soc.* **140**, 155–158 (2018).
24. Miura, Y., Oka, H., Yamano, E. & Morita, M. Convenient deuteration of bromo aromatic compounds by reductive debromination with sodium amalgam in CH_3OD. *J. Org. Chem.* **62**, 1188–1190 (1997).
25. Wang, X. et al. General and practical potassium methoxide/disilane-mediated dehalogenative deuteration of (hetero)arylhalides. *J. Am. Chem. Soc.* **140**, 10970–10974 (2018).
26. Munz, D. et al. Proton or metal? The H/D exchange of arenes in acidic solvents. *ACS Catal.* **5**, 769–775 (2015).
27. Atzrodt, J., Derdau, V., Kerr, W. J. & Reid, M. C–H functionalisation for hydrogen isotope exchange. *Angew. Chem. Int. Ed.* **57**, 3022–3047 (2018).
28. Atzrodt, J., Derdau, V., Fey, T. & Zimmermann, J. The renaissance of H/D exchange. *Angew. Chem. Int. Ed.* **46**, 7744–7765 (2007).
29. Yu, R. P., Hesk, D., Rivera, N., Pelczer, I. & Chirik, P. J. Iron-catalysed tritiation of pharmaceuticals. *Nature* **529**, 195–199 (2016).
30. Loh, Y. Y. et al. Photoredox-catalyzed deuteration and tritiation of pharmaceutical compounds. *Science* **358**, 1182–1187 (2017).
31. Li, W. et al. Scalable and selective deuteration of (hetero)arenes. *Nat. Chem.* **14**, 334–341 (2022).
32. Martins, A. & Lautens, M. A simple, cost-effective method for the regioselective deuteration of anilines. *Org. Lett.* **10**, 4351–4353 (2008).
33. Wang, L., Xia, Y., Derdau, V. & Studer, A. Remote site-selective radical $C(sp^3)$–H monodeuteration of amides using D_2O. *Angew. Chem. Int. Ed.* **60**, 18645–18650 (2021).
34. Jia, Z. & Luo, S. Visible light promoted direct deuteration of alkenes via Co(III)–H mediated H/D exchange. *CCS Chem.* **5**, 1069–1076 (2023).
35. Li, R. et al. One-pot H/D exchange and low-coordinated iron electrocatalyzed deuteration of nitriles in D_2O to α,β-deuterio aryl ethylamines. *Nat. Commun.* **13**, 5951–5963 (2022).
36. Li, N. et al. Highly selective single and multiple deuteration of unactivated $C(sp^3)$–H bonds. *Nat. Commun.* **13**, 4224–4232 (2022).
37. He, T., Klare, H. F. T. & Oestreich, M. Perdeuteration of deactivated aryl halides by H/D exchange under superelectrophile catalysis. *J. Am. Chem. Soc.* **144**, 4734–4738 (2022).
38. Song, H. et al. Remote site-selective $C(sp^3)$–H monodeuteration of unactivated alkenes via chain-walking strategy. *ACS Catal.* **13**, 3644–3654 (2023).
39. Xu, H., Jiang, Z.-J., Gao, Z., Chen, J. & Gao, K. H/D exchange of aromatic sulfones via base promotion and silver catalysis. *J. Org. Chem.* **89**, 8468–8477 (2024).
40. Ni, Y. et al. Hexafluorophosphate-triggered hydrogen isotope exchange (HIE) in fluorinated environments: a platform for the deuteration of aromatic compounds via strong bond activation. *Angew. Chem. Int. Ed.* **64**, e202417889 (2025).
41. Tao, Y. et al. Deuteration of arenes in pharmaceuticals via photo-induced solvated electrons. *Chem* **10**, 3374–3384 (2024).
42. Kerr, W. J., Reid, M. & Tuttle, T. Iridium-catalyzed C–H activation and deuteration of primary sulfonamides: an experimental and computational study. *ACS Catal.* **5**, 402–410 (2015).
43. Ma, S., Villa, G., Thuy-Boun, P. S., Homs, A. & Yu, J.-Q. Palladium-catalyzed *ortho*-selective C–H deuteration of arenes: evidence for superior reactivity of weakly coordinated palladacycles. *Angew. Chem. Int. Ed.* **53**, 734–737 (2014).
44. Farizyan, M., Mondal, A., Mal, S., Deufel, F. & van Gemmeren, M. Palladium-catalyzed nondirected late-stage C–H deuteration of arenes. *J. Am. Chem. Soc.* **143**, 16370–16376 (2021).
45. Dey, J., Kaltenberger, S. & van Gemmeren, M. Palladium(II)-catalyzed nondirected late-stage $C(sp^2)$–H deuteration of heteroarenes enabled through a multi-substrate screening approach. *Angew. Chem. Int. Ed.* **63**, e202404421 (2024).
46. Du, H.-Z., Li, J., Maron, L., Shi, Z.-J. & Guan, B.-T. Directed aromatic deuteration and tritiation of pharmaceuticals by heavy alkali metal amide catalysts. *ACS Catal.* **14**, 9640–9647 (2024).
47. Guo, L. et al. Cascade alkylation and deuteration with aryl iodides via Pd/norbornene catalysis: an efficient method for the synthesis of congested deuterium-labeled arenes. *Chem. Commun.* **55**, 8567–8570 (2019).
48. Lang, Y., Peng, X., Li, C.-J. & Zeng, H. Photoinduced catalyst-free deborylation–deuteration of arylboronic acids with D_2O. *Green. Chem.* **22**, 6323–6327 (2020).
49. Lee, C.-Y., Ahn, S.-J. & Cheon, C.-H. Protodeboronation of ortho- and para-phenol boronic acids and application to *ortho* and *meta* functionalization of phenols using boronic acids as blocking and directing groups. *J. Org. Chem.* **78**, 12154–12160 (2013).
50. Lozada, J., Liu, Z. & Perrin, D. M. Base-promoted protodeboronation of 2,6-disubstituted arylboronic acids. *J. Org. Chem.* **79**, 5365–5368 (2014).
51. Ahn, S.-J., Lee, C.-Y., Kim, N.-K. & Cheon, C.-H. Metal-free protodeboronation of electron-rich arene boronic acids and its application to ortho-functionalization of electron-rich arenes using a boronic acid as a blocking group. *J. Org. Chem.* **79**, 7277–7285 (2014).
52. Zhao, D., Petzold, R., Yan, J., Muri, D. & Ritter, T. Tritiation of aryl thianthrenium salts with a molecular palladium catalyst. *Nature* **600**, 444–449 (2021).
53. Li, Y. et al. Organophotocatalytic selective deuterodehalogenation of aryl or alkyl chlorides. *Nat. Commun.* **12**, 2894–2906 (2021).
54. Li, N., Li, Y., Wu, X., Zhu, C. & Xie, J. Radical deuteration. *Chem. Soc. Rev.* **51**, 6291–6306 (2022).
55. Zhao, D. & Ritter, T. Illuminating aromatic deuteration. *Chem* **10**, 3266–3278 (2024).
56. Liu, C. et al. Controllable deuteration of halogenated compounds by photocatalytic D_2O splitting. *Nat. Commun.* **9**, 80–89 (2018).
57. Zhang, B. & Yu, Y. photocatalytic deuteration of halides using D_2O over CdSe porous nanosheets: a mild and controllable route to deuterated molecules. *Angew. Chem. Int. Ed.* **57**, 5590–5592 (2018).
58. He, M., Li, R., Cheng, C., Liu, C. & Zhang, B. Microenvironment regulation breaks the Faradaic efficiency-current density trade-off for electrocatalytic deuteration using D_2O. *Nat. Commun.* **15**, 5231–5240 (2024).
59. Liu, S. et al. Catalyst-free decarboxylative deuteration using tailored photoredox-active carboxylic acids. *Green. Chem.* **26**, 10456–10462 (2024).
60. Xu, Y. et al. Selective monodeuteration enabled by bisphosphonium catalyzed ring opening processes. *Nat. Commun.* **15**, 9366–9374 (2024).
61. Hu, A., Guo, J.-J., Pan, H. & Zuo, Z. Selective functionalization of methane, ethane, and higher alkanes by cerium photocatalysis. *Science* **361**, 668–672 (2018).
62. Lu, L., Li, H., Zheng, Y., Bu, F. & Lei, A. Facile and economical electrochemical dehalogenative deuteration of (hetero)aryl halides. *CCS Chem.* **3**, 2669–2675 (2021).
63. Liu, C., Han, S., Li, M., Chong, X. & Zhang, B. Electrocatalytic deuteration of halides with D_2O as the deuterium source over a copper nanowire arrays cathode. *Angew. Chem. Int. Ed.* **59**, 18527–18531 (2020).
64. Li, P. et al. Facile and general electrochemical deuteration of unactivated alkyl halides. *Nat. Commun.* **13**, 3774–3782 (2022).
65. Zhao, Z. et al. Electrochemical C–H deuteration of pyridine derivatives with D_2O. *Nat. Commun.* **15**, 3832–3840 (2024).
66. Cheng, J. & Cheng, X. Electrochemical monodeuterodefluorination of trifluoromethyl aromatic compounds with deuterium oxide. *CCS Chem.* **6**, 230–240 (2024).

67. Chen, Y.-J. et al. Selective dearomatic deuteration of (het)arenes via electrophotocatalysis. *CCS Chem.* **7**, 1289–1296 (2025).
68. He, M. et al. Boron clusters as efficient shuttles for electrocatalytic deuterium labelling via radical H/D exchange. *Nat. Catal.* **8**, 784–793 (2025).
69. Bu, F. et al. Electrocatalytic reductive deuteration of arenes and heteroarenes. *Nature* **634**, 592–599 (2024).
70. Qu, R. et al. Mechanical-force-induced non-spontaneous dehalogenative deuteration of aromatic iodides enabled by using piezoelectric materials as a redox catalyst. *Angew. Chem. Int. Ed.* **63**, e202400645 (2024).
71. Zhang, J. et al. Mechanochemical nickel-catalyzed dechlorination-deuteration of aryl chlorides via piezoelectric-promoted Ar–Zn–X intermediates. *ACS Catal.* **15**, 14794–14804 (2025).
72. Kopf, S. et al. Recent developments for the deuterium and tritium labeling of organic molecules. *Chem. Rev.* **122**, 6634–6718 (2022).
73. Li, H., Shabbir, M., Li, W. & Lei, A. Recent advances in deuteration reactions. *Chin. J. Chem.* **42**, 1145–1156 (2024).
74. Kuriyama, M. et al. Deuterodechlorination of Aryl/Heteroaryl Chlorides Catalyzed by a Palladium/Unsymmetrical NHC System. *J. Org. Chem.* **81**, 8934–8946 (2016).
75. Kameo, H. et al. Palladium–borane cooperation: evidence for an anionic pathway and it's application to catalytic hydro-/deuterodechlorination. *Angew. Chem. Int. Ed.* **58**, 18783–18787 (2019).
76. Li, J. et al. Homogenous palladium-catalyzed dehalogenative deuteration and tritiation of aryl halides with D_2/T_2 Gas. *J. Am. Chem. Soc.* **146**, 31497–31506 (2024).
77. Wang, M., Pang, W. H., Yuen, O. Y., Ng, S. S. & So, C. M. Palladium-catalyzed deuterodehalogenation of halogenated aryl triflates using isopropanol-d8 as the deuterium source. *Org. Lett.* **25**, 8429–8433 (2023).
78. Zhang, H. H., Bonnesen, P. V. & Hong, K. Palladium-catalyzed Br/D exchange of arenes: selective deuterium incorporation with versatile functional group tolerance and high efficiency. *Org. Chem. Front.* **2**, 1071–1075 (2015).
79. Lemus, M. S. L. et al. Nickel-catalyzed hydro- and deuterodehalogenations of (hetero)aryl halides under aqueous micellar catalysis conditions. *ChemSusChem* **18**, e202500043 (2025).
80. Li, W. et al. Copper-catalysed low-temperature water–gas shift reaction for selective deuteration of aryl halides. *Chem. Sci.* **12**, 14033–14038 (2021).
81. Sahoo, B. et al. A biomass-derived non-noble cobalt catalyst for selective hydrodehalogenation of alkyl and (hetero)aryl halides. *Angew. Chem. Int. Ed.* **56**, 11242–11247 (2017).
82. Chen, B.-Z. et al. Cobalt-catalyzed dehalogenative deuterations with D_2O. *Chin. J. Catal.* **59**, 250–259 (2024).
83. Chen, Y. et al. Pd-catalyzed deuteration of aryl halides with deuterium oxide. *Nat. Commun.* **16**, 2584–2590 (2025).
84. Song, S. et al. DMSO-catalysed late-stage chlorination of (hetero) arenes. *Nat. Catal.* **3**, 107–115 (2020).
85. Wang, W. et al. Catalytic electrophilic halogenation of arenes with electron withdrawing substituents. *J. Am. Chem. Soc.* **144**, 13415–13425 (2022).
86. Würtz, S., Rakshit, S., Neumann, J. J., Dröge, T. & Glorius, F. Palladium-catalyzed oxidative cyclization of N-aryl enamines from anilines to indoles. *Angew. Chem. Int. Ed.* **47**, 7230–7233 (2008).
87. Pierson, C. N. & Hartwig, J. F. Mapping the mechanisms of oxidative addition in cross-coupling reactions catalysed by phosphine-ligated Ni(0). *Nat. Chem.* **16**, 930–937 (2024).
88. Everson, D. A., Jones, B. A. & Weix, D. J. Replacing conventional carbon nucleophiles with electrophiles: nickel-catalyzed reductive alkylation of aryl bromides and chlorides. *J. Am. Chem. Soc.* **134**, 6146–6159 (2012).
89. Liu, Q. et al. Revealing a second transmetalation step in the Negishi coupling and its competition with reductive elimination: improvement in the interpretation of the mechanism of biaryl syntheses. *J. Am. Chem. Soc.* **131**, 10201–10210 (2009).
90. Biswas, S. & Weix, D. J. Mechanism and selectivity in nickel-catalyzed cross-electrophile coupling of aryl halides with alkyl halides. *J. Am. Chem. Soc.* **135**, 16192–16197 (2013).
91. Sakai, M. et al. Metallic nickel-catalyzed reduction of aryl halides with zinc powder and ethanol. *B. Chem. Soc. Jpn.* **65**, 1739–1740 (1992).
92. Huang, H., Alvarez-Hernandez, J. L., Hazari, N., Mercado, B. Q. & Uehling, M. R. Effect of 6,6′-substituents on bipyridine-ligated Ni catalysts for cross-electrophile coupling. *Acs. Catal.* **14**, 6897–6914 (2024).
93. Tang, T. et al. Interrogating the mechanistic features of Ni(I)-mediated aryl iodide oxidative addition using electroanalytical and statistical modeling techniques. *J. Am. Chem. Soc.* **145**, 8689–8699 (2023).
94. Dawson, G. A., Lin, Q., Neary, M. C. & Diao, T. Ligand redox activity of organonickel radical complexes governed by the geometry. *J. Am. Chem. Soc.* **145**, 20551–20561 (2023).
95. Lin, Q. & Diao, T. Mechanism of Ni-catalyzed reductive 1,2-dicarbofunctionalization of alkenes. *J. Am. Chem. Soc.* **141**, 17937–17948 (2019).
96. Zhao, Y., Huo, L., Zhao, X. & Chu, L. Atroposelective three-component (fluoro)methylative alkylation of terminal alkynes. *ACS Catal.* **15**, 63–71 (2025).
97. He, R.-D. et al. Reductive alkylation of alkenyl acetates with alkyl bromides by nickel catalysis. *Angew. Chem. Int. Ed.* **61**, e202114556 (2022).
98. Li, X. et al. Nickel-catalyzed stereoselective cascade C–F functionalizations of *gem*-difluoroalkenes. *ACS Catal.* **13**, 2135–2141 (2023).

Acknowledgements

We thank the financial support from National Natural Science Foundation of China (No. 22001147), Taishan Scholars Project of Shandong Province (No. tsqn202103027), Distinguished Young Scholars of Shandong Province (Overseas) (No. 2022HWYQ-001), and Qilu Youth Scholar Funding of Shandong University.

Author contributions

Y.-Q.G., T.-Z.W. and X.-R.T. conducted and analysed the experiments. Y.-Q.G. and M.B. prepared the Supplementary Information. L.A. and Y.-F.L. directed the project and wrote the manuscript with contributions from all co-workers. All authors discussed the results and commented on the manuscript.

Competing interests

The authors declare no competing interests.

Additional information

Supplementary information The online version contains supplementary material available at https://doi.org/10.1038/s41467-025-66569-z.

Correspondence and requests for materials should be addressed to Lutz Ackermann or Yu-Feng Liang.

Peer review information *Nature Communications* thanks the anonymous reviewers for their contribution to the peer review of this work. A peer review file is available.